

Global transcriptomic profiling of aspen trees under elevated [CO₂] to identify potential molecular mechanisms responsible for enhanced radial growth

Hairong Wei · Jiqing Gou · Yordan Yordanov ·
Huaxin Zhang · Ramesh Thakur · Wendy Jones ·
Andrew Burton

Received: 17 July 2012 / Accepted: 7 September 2012
© The Botanical Society of Japan and Springer Japan 2012

Abstract Aspen (*Populus tremuloides*) trees growing under elevated [CO₂] at a free-air CO₂ enrichment (FACE) site produced significantly more biomass than control trees. We investigated the molecular mechanisms underlying the observed increase in biomass by producing transcriptomic profiles of the vascular cambium zone (VCZ) and leaves, and then performed a comparative study to identify significantly changed genes and pathways after 12 years exposure to elevated [CO₂]. In leaves, elevated [CO₂] enhanced expression of genes related to Calvin cycle activity and linked pathways. In the VCZ, the pathways involved in cell growth, cell division, hormone metabolism, and secondary cell wall formation were altered while auxin conjugation, ABA synthesis, and cytokinin

glucosylation and degradation were inhibited. Similarly, the genes involved in hemicellulose and pectin biosynthesis were enhanced, but some genes that catalyze important steps in lignin biosynthesis pathway were inhibited. Evidence from systemic analysis supported the functioning of multiple molecular mechanisms that underpin the enhanced radial growth in response to elevated [CO₂].

Keywords Carbon dioxide · Aspen · Transcriptome · Vascular cambium zone · Leaves

Electronic supplementary material The online version of this article (doi:10.1007/s10265-012-0524-4) contains supplementary material, which is available to authorized users.

H. Wei (✉) · J. Gou · Y. Yordanov · R. Thakur · W. Jones ·
A. Burton (✉)
School of Forest Resources and Environmental Science,
Michigan Technological University, 1400 Townsend Drive,
Houghton, MI 49931, USA
e-mail: hairong@mtu.edu

A. Burton
e-mail: ajburton@mtu.edu

H. Wei
Department of Computer Science, Michigan Technological
University, 1400 Townsend Drive, Houghton, MI 49931, USA

H. Wei
Biotechnology Research Center, Michigan Technological
University, 1400 Townsend Drive, Houghton, MI 49931, USA

H. Zhang
Research Institute of Forestry, Chinese Academy of Forestry,
Beijing 100091, China

Introduction

Atmospheric CO₂ concentration has risen some 35–40 % since preindustrial times, and 23 % since 1959. Elevated [CO₂] has been shown to have significant effects on tree growth because CO₂ is one of the substrates required for photosynthesis. A twelve-year experiment conducted at the Aspen FACE (free-air CO₂ enrichment) site near Rhineland, Wisconsin, USA has demonstrated that the enhancement of CO₂ levels can increase growth of aspen (*Populus tremuloides*) trees by up to 31 % in height or diameter, and 60 % in aboveground volume (Kubiske et al. 2007), depending on the genotype. Significant increase also occurs in fine root biomass (Pregitzer et al. 2008). The enhanced growth was accompanied by increases in light-saturated photosynthesis of 30–85 % for upper canopy leaves, with no acclimation in the response occurring from 2000 through 2008 (Darbah et al. 2010; Uddling et al. 2008). Elevated [CO₂] can have a variety of physiological and ecological effects on plants, including improvements in nitrogen and water use efficiency (Leakey et al. 2009; Li et al. 2003), stimulation of dark respiration (Barbehenn et al. 2004; Leakey et al. 2009), alteration of plant nutrient

content and plant–insect interactions (Hillstrom and Lindroth 2008), and altered decomposition of roots and aboveground litter (Angelis et al. 2004; Liu et al. 2005, 2009b). Growth under elevated $[\text{CO}_2]$ can reduce drought stress by increasing water use efficiency (Conley et al. 2001; Li et al. 2008); however, it is not clear if long-term CO_2 fumigation can alter overall water consumption (Chen et al. 2006; Orcutt et al. 2000; Tuba and Lichtenthaler 2007).

To understand the molecular mechanisms underpinning significant enhancement tree growth under elevated $[\text{CO}_2]$, we have examined the mid-growing season transcriptome profiles of two tissues types, leaves and the vascular cambium zone (VCZ), at the same time using Affymetrix Poplar Whole Genome Arrays. These arrays contain 61413 features, including 61252 poplar design sequences collected from the *Populus trichocarpa* genome project (Tuskan et al. 2006), and other poplar sequences present in Genbank (Benson et al. 1993). These genome-wide microarray chips allowed us to generate informative results from which we could draw a more holistic picture of the transcriptional events and regulation occurred in aspen trees growing under elevated $[\text{CO}_2]$.

Several previous studies were conducted to identify the genes that were responsive to elevated $[\text{CO}_2]$ in *Populus* leaves (Druart et al. 2006; Gupta et al. 2005; Taylor et al. 2005). Gupta et al. (2005) used cDNA arrays containing only 4,600 ESTs and focused on the effect of O_3 and the interaction between CO_2 and O_3 . They were able to show 216 genes that were responsive to elevated $[\text{CO}_2]$. Taylor et al. (2005) used POP1 and POP2 arrays containing 13,488 and 24,735 probes, respectively. The study by Druart et al.

(2006) also used POP1 arrays, but interrogated genes expression from both leaves and the VCZ of stems of *Populus deltoides*. However, the VCZ tissues they used differed from those in this study in that they were harvested at regions fairly close (15–25 cm) to the apical meristems of coppice trees and were harvested in November when the trees might approach winter dormancy.

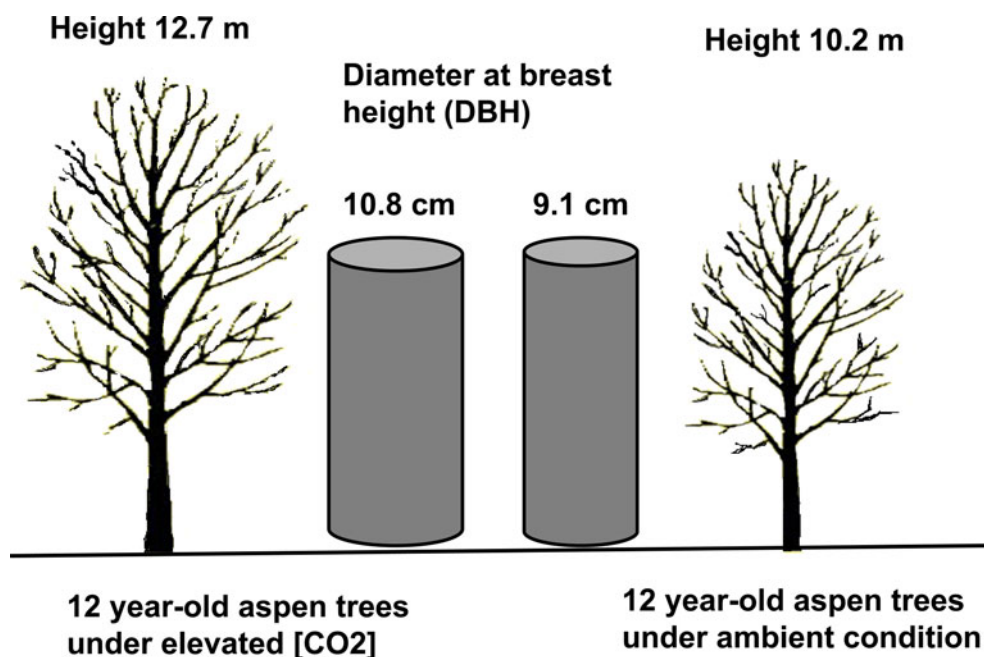
In the present study, we used genome-wide microarrays and focused primarily on leaves at about $\frac{1}{4}$ distance of canopy height from highest apical meristem, and lower stem VCZ tissues of 12-year-old aspen trees to identify significantly altered genes, and gene sets as well as possible molecular mechanisms underpinning the increased radial growth observed in response to elevated $[\text{CO}_2]$. The research employed a number of bioinformatics analyses that included genome-wide homology gene mapping between poplar and Arabidopsis, multiple statistical analyses for identifying differentially expressed genes (DEGs), genome-wide protein domain and GO enrichment analysis, and large-scale pathway analysis. This allowed a more comprehensive biological examination and interpretation for revealing new information of the influence of elevated $[\text{CO}_2]$ on the transcriptional activity of many biological pathways and biological processes related to growth.

Results

Identification of DEGs in leaves and VCZ

Raw microarray data generated from 12 years old aspen trees grown under elevated $[\text{CO}_2]$ and control conditions

Fig. 1 Average sizes of harvested aspen trees grown in elevated $[\text{CO}_2]$ and ambient conditions



with distinct discrepancies in growth (Fig. 1) were first normalized with robust multichip average (RMA) algorithm (Irizarry et al. 2003) and then were analyzed by rank product (RP) (Breitling et al. 2004) method to identify 1961 and 539 DEGs in VCZ and leaves. Some of these were summarized in Table 1. One of the significant discoveries from the microarray analysis was the up-regulation of genes whose functions are closely associated with cell loosening and expansion in VCZ tissues. For example, seven genes encoding glycosyl hydrolases were up-regulated in VCZ, with an increase between 60.4 and 121.1 % (Table 1). These enzymes function primarily to cleave the xyloglucan hemicellulose cross-linking chains that exist between cellulose microfibrils, leading to cell wall loosening (Cosgrove 2000). In addition to genes encoding glycosyl hydrolases, several other genes involved in modifying cell wall extensibility also increased in VCZ in response to elevated [CO₂]. These included five expansins, all of which had at least 5 and up to more than 100 times higher expression in VCZ than leaves and three pectin esterases (Derbyshire et al. 2007) that are known to modify of cell wall rigidity during cell expansion and division (Derbyshire et al. 2007; Kutschera 1990), increased between 89.9 and 306.6 %.

Examination of gene lists for genes involved in the cell cycle revealed 13 genes that were up-regulated in response to elevated [CO₂]. For example, genes XM_002304135 (cyclin A2;3), XM_002326989 (cyclin P4;1), XM_002298096 (cyclase associated protein (CAP)), XM_002313980 (CYC3B cyclin-dependent protein kinase), and XM_002307755 (CYCB2;3 cyclin-dependent protein kinase regulator), increased 64.5, 80.6, 37.9, 25.2 and 35.2 %, respectively, in the VCZ (Table 1), potentially promoting cell division through both G1 → S and G2 → M transitions, as similar genes have been known to do so (Cooper and Strich 2002; Ji et al. 2005; Joubes et al. 2001; Yu et al. 2003). Recently, the increased expression of the auxin carrier LAX3 was reported to induce of cell wall remodeling enzymes (Swarup et al. 2008). Our data revealed that two LAX3 genes increased 178.0 and 100.5 % in VCZ in response to elevated [CO₂], and one auxin influx carrier gene, XM_002312937, increased 43 % while several genes that promote the formation of IAA-amino acid conjugate decreased in response to elevated [CO₂]. In addition, several genes involved in ABA biosynthesis and response were down-regulated while the gene, XM_002301149, CYP707A4, involved in ABA catabolism (Okamoto et al. 2006, 2011), increased 74.6 % in VCZ. Taken together, evidence tends to support that elevated [CO₂] can directly or indirectly drive cell division and expansion in VCZ.

Theoretically, cell division and expansion require the formation of new cell walls. Therefore, the genes encoding cellulose synthases, beta-xylosidase 1 and 2 (secondary cell

wall hemicellulose metabolism; Goujon et al. 2003), UDP-L-rhamnose synthase, UDP-glucuronate 4-epimerase, UDP-arabinose 4-epimerase, UDP-glucose dehydrogenases (UGD), laccases and two transcription factors, XM_002299908 (MYB46) and XM_002309877 (MYB69) that are known to regulate cell wall biosynthesis (Zhong et al. 2008), were significantly upregulated in VCZ. In the VCZ, the up-regulation of six clathrin adaptor genes and one clathrin assembly gene suggests that intracellular protein transport was enhanced during CO₂ fumigation.

Interestingly, the gene Cesa7 encoding cellulose synthase was up-regulated 110.0 % in response to elevated [CO₂] (Table 1). Two other genes, Cesa 4 and Cesa8, which are generally required for secondary cell wall biosynthesis were up-regulated 7.5 and 23.4 % (Table 1) respectively in VCZ. Two genes encoding UDP-glucose-4-epimerase, and one encoding UDP-glucuronate 4-epimerase, were up-regulated 42.8–84.0 %. UDP-glucose-4-epimerase is responsible for the interconversion of UDP-D-glucose and UDP-D-galactose. UDP-D-glucose is the precursor for sucrose, α-D-glucose 1-phosphate, UDP-L-rhamnose, and UDP-D-glucuronate. UDP-D-glucuronate, in turn, is the precursor for UDP-D-xylose and UDP-D-galacturonate. UDP-glucuronate 4-epimerase is an enzyme that catalyzes the formation of UDP-D-galacturonate from UDP-glucuronate.

As structural components of cells, microtubules are involved in many cellular processes including mitosis (Gregory et al. 2008), cytokinesis (Canman et al. 2000; Larkin and Danilchik 1999; Surka et al. 2002), and vesicular transport (Hamm-Alvarez and Sheetz 1998). We observed an increased VCZ-specific expression of seven microtubule genes (Table 1) in the VCZ of CO₂ treated trees, which suggests the deployment of microtubules in cell division. In addition, expression levels of five genes encoding the kinesin motor were 28–52 % higher in VCZ of CO₂ treated trees than in control trees, suggesting that microtubule-based vesicle transport was possibly driven by kinesin, which is known to move along microtubule cables and is powered by the hydrolysis of ATP (Muto et al. 2005; Schnitzer and Block 1997). Expression of two genes, XM_002299432 and XM_002318256, which encode dynamitin-like protein, increased 70.8 and 22.8 %, respectively, in VCZ in response to elevated [CO₂]. These pieces of evidence suggest an augmented cell growth and division in the VCZ of CO₂ treated trees as compared to control trees.

The up- and down-regulation of genes encoding cytokinin oxidase suggest the metabolism of cytokinins was impacted due to the elevated [CO₂]. What also changed is the activity of cytokinin transporters. For instance, XM_002301034 and XM_002307315 encoding homologs of PUP3, and PUP2, respectively, were down-regulated 121.1 and 18.8 %, respectively in VCZ. Four genes,

Table 1 DEGs in response to elevated [CO₂]

Probe	Genbank ID	Description	FC	EXP _{V/L}	Poplar V2.0 ID
PtpAffx.132592.1.S1_at	XM_002313646 ^a	EXLA2 (expansin-like A2)	2.26	>5	–
Ptp.6656.1.S1_s_at	XM_002312217 ^a	EXPA1 (expansin A1)	1.97	>10	–
Ptp.584.1.A1_at	XM_002320365 ^a	EXGT-A4 (endoxyloglucan transferase a4);	2.68	>10	POPTR_0006s19310
Ptp.5980.3.A1_a_at	XM_002309337 ^a	Expansin-related protein 3 precursor	1.45	>100	POPTR_0004s18840
Ptp.617.1.S1_at	XM_002305509 ^a	EXLA1 (expansin-like A1)	2.03	>100	POPTR_0008s13200
PtpAffx.144673.1.S1_s_at	XM_002326285 ^a	Pectinesterase	1.92	>5	POPTR_0006s13670
PtpAffx.132383.1.A1_s_at	XM_002326285 ^a	Pectinesterase	1.89	>10	POPTR_0006s13670
Ptp.144.1.S1_at	–	ATPME3; pectinesterase	4.06	>25	–
PtpAffx.18355.1.S1_at	XM_002308836	CYC1BAT; cyclin-dep. protein kinase regulator	1.24	>5	–
PtpAffx.214175.1.S1_x_at	XM_002324798	CYC3B cyclin-dep. protein kinase regulator	1.30	>5	–
PtpAffx.200516.1.S1_at	XM_002298096	CYCA2;3 cyclin-dep. protein kinase regulator	1.38	>25	POPTR_0001s17730
PtpAffx.200879.1.S1_at	XM_002298415	CYCB1;4 cyclin-dep. protein kinase regulator	1.29	>10	POPTR_0001s27890
PtpAffx.204823.1.S1_at	XM_002313980	CYCB1;4 cyclin-dep. protein kinase regulator	1.25	>10	POPTR_0009s07100
Ptp.5638.1.S1_at	XM_002307755	CYCB2;3 cyclin-dep. protein kinase regulator	1.35	>10	–
Ptp.6857.2.S1_s_at	XM_002312770	CYCB2;4 cyclin-dep. protein kinase regulator	1.22	>5	POPTR_0009s16730
PtpAffx.147539.1.A1_at	–	CYCB2;4 cyclin-dep. protein kinase regulator	1.07	>2	–
PtpAffx.164104.1.S1_s_at	XM_002316115	CYCB3;1 cyclin-dep. protein kinase	1.27	>2	–
PtpAffx.56737.2.A1_a_at	XM_002319084	CDC20.2; signal transducer	1.41	>25	POPTR_0019s03850–
Ptp.2922.1.S1_at	XM_002313014	cyclin cyclase associated (CAP)	1.16	>5	POPTR_0003s05690
PtpAffx.202922.1.S1_at	XM_002304135	CYCA2;3 (cyclin A2;3);	1.64	>10	POPTR_0014s04930
PtpAffx.144614.1.S1_at	XM_002326989 ^a	CYCP4;1 (cyclin p4;1);	1.81	>100	–
PtpAffx.46431.1.S1_at	XM_002311482 ^a	GH9B1 glycosyl hydrolase 9B1 (cellulose)	2.08	>5	POPTR_0008s13200
PtpAffx.6557.1.A1_at	XM_002311482 ^a	GH9B1 glycosyl hydrolase 9B1 (cellulose)	1.84	>20	–
Ptp.2717.2.S1_s_at	XM_002311482 ^a	GH9B6 glycosyl hydrolase 9B6	1.87	>25	–
Ptp.6339.1.S1_s_at	XM_002328213	Glycosyl hydrolase family 17 protein	1.96	>2	–
PtpAffx.2710.3.S1_at	XM_002300469	Glycosyl hydrolase family 17 protein	1.60	>10	POPTR_0001s45320
PtpAffx.204306.1.S1_at	XM_002306147	Glycosyl hydrolase family 35 protein	1.90	>5	POPTR_0004s18070
PtpAffx.203068.1.S1_at	XM_002303369	Glycosyl hydrolase family 38 protein	2.21	>2	POPTR_0007s09730
Ptp.6069.1.S1_a_at	XM_002320147 ^a	GH3 family protein	–2.61	<–5	–
Ptp.6069.2.S1_a_at	XM_002320147 ^a	GH3 family protein	–2.26	<–2	–
PtpAffx.72392.1.A1_at	XM_002300212 ^a	GH3.3; indole-3-acetic acid amido synthetase	–2.35	>5	–
PtpAffx.132894.1.S1_a_at	XM_002301363 ^a	GH3 family protein	–1.84	<–2	POPTR_0002s16960
Ptp.4793.1.S1_at	XM_002302195 ^a	ILL6; IAA-amino acid conjugate hydrolase	–2.34	>1	–
PtpAffx.100235.1.S1_s_at	XM_002302217 ^a	LAX3 (LIKE AUX1 3); auxin influx transporter	2.78	>25	POPTR_0002s08750
PtpAffx.25167.2.A1_at	– ^a	LAX3 (LIKE AUX1 3); auxin influx transporter	2.00	>4	–
PtpAffx.17419.1.A1_at	XM_002312937 ^a	Auxin influx carrier component	1.43	>25	–
PtpAffx.204148.1.S1_at	XM_002305335 ^a	PIN8 auxin:hydrogen symporter	–2.22	>2	–
PtpAffx.97482.1.S1_at	XM_002320273 ^a	BXL1 (BETA-XYLOSIDASE 1); hydrolase,	2.10	>20	POPTR_0014s11730
PtpAffx.202369.1.S1_at	XM_002302723 ^a	BXL2 (BETA-XYLOSIDASE 2); hydrolase,	1.92	>20	POPTR_0002s19830
PtpAffx.14026.1.S1_s_at	XM_002316779 ^a	Cellulose synthase	1.71	>100	–
PtpAffx.5943.1.A1_at	XM_002308376 ^a	CesA7 (IRX3); cellulose synthase	2.10	>5	–
Ptp.666.1.S1_at	XM_002301820	CesA4 cellulose synthase A4	1.08	>25	–
Ptp.296.1.S1_at	XM_002305024	CesA8 cellulose synthase A8	1.23	>25	–
Ptp.3250.1.S1_s_at	XM_002322676	CesA3 cellulose synthase A3	1.07	>10	POPTR_0014s12000
PtpAffx.157368.1.S1_s_at	XM_002303309 ^a	UTP–glucose-1-phosphate uridylyltransferase	2.15	>5	–
PtpAffx.70110.1.A1_at	XM_002301244 ^a	GAE3 UDP-glucuronate 4-epimerase	1.84	>5	POPTR_0002s14750
PtpAffx.103875.1.S1_at	XM_002318144 ^a	GUT1; glucuronoxylan	1.97	>2	–
Ptp.126.1.S1_s_at	XM_002306028	UDP-glucose 4-epimerase	1.43	>5	–

Table 1 continued

Probe	Genbank ID	Description	FC	EXP _{V/L}	Poplar V2.0 ID
Ptp.3953.1.S1_s_at	XM_002304442	UDP-glucose 4-epimerase	1.79	>2	POPTR_0003s12380
PtpAffx.147946.1.S1_at	– ^a	RHM3 (UDP-L-rhamnose synthase)	1.69	>2	–
PtpAffx.59601.1.S1_a_at	XM_002317651 ^a	MUR4 (UDP-arabinose 4-epimerase)	2.17	>1	–
PtpAffx.137959.1.S1_at	XM_002308172 ^a	IRX12 (IRREGULAR XYLEM 12); laccase	2.04	>5	–
Ptp.6345.1.S1_s_at	XM_002308172 ^a	IRX12 (IRREGULAR XYLEM 12); laccase	1.42	>25	POPTR_0016s11950
Ptp.1855.1.S1_at	XM_002308172 ^a	Laccase 1C	1.65	>25	–
PtpAffx.5154.1.A1_s_at	XM_002325536 ^a	LAC1 (Laccase 1); laccase	–3.50	>10	POPTR_0019s11820
PtpAffx.162923.1.S1_s_at	XM_002312150 ^a	LAC12 (laccase 12); laccase	2.14	>100	POPTR_0008s07370
PtpAffx.44574.1.A1_at	XM_002315095 ^a	LAC12 (laccase 12); laccase	2.10	>25	–
Ptp.6122.1.A1_at	XM_002317469 ^a	LAC17 (laccase 17); laccase	1.44	>25	–
PtpAffx.224175.1.S1_s_at	XM_002299908 ^a	MYB46 (MYB DOMAIN PROTEIN 46);	1.77	>5	POPTR_0001s27430
PtpAffx.207054.1.S1_at	XM_002309877 ^a	MYB69 (MYB DOMAIN PROTEIN 69);	1.71	>5	POPTR_0007s04140
Ptp.6393.1.S1_at	XM_002324067 ^a	UDP-glucose 6-dehydrogenase,	1.95	>2	None
PtpAffx.29653.1.S1_s_at	XM_002306028 ^a	UDP-glucose 6-dehydrogenase,	1.82	>2	POPTR_0017s12760
Ptp.2708.1.S1_at	XM_002311295 ^a	UDP-glucose 6-dehydrogenase,	1.82	>25	None
PtpAffx.55460.2.S1_a_at	XM_002302640 ^a	OMT1 caffeate O-methyltransferase	–1.81	>10	POPTR_0002s18150
PtpAffx.34384.1.S1_s_at	XM_002327918 ^a	4-coumarate-coa ligase (4LC)	–3.86	>1	POPTR_0017s06210
PtpAffx.12056.3.S1_a_at	XM_002325779	4-coumarate-coa ligase (4LC)	–1.42	<–5	POPTR_0019s07600
Ptp.3043.1.S1_s_at	XM_002297663	4-coumarate-coa ligase (4LC)	–1.02	>5	POPTR_0001s07400
PtpAffx.141260.2.A1_at	XM_002317802	Caffeic acid 3-O-methyltransferase	1.79	>25	–
Ptp.4675.1.S1_s_at	XM_002308824	CYP98.1	1.45	>2	POPTR_0006s03180
PtpAffx.220781.1.S1_at	XM_002332733	CPY71B35	1.01	<–1	POPTR_0007s06350
Ptp.7180.2.S1_s_at	XM_002309241	Rhomboid family protein	1.51	>2	POPTR_0006s21220
PtpAffx.200787.1.S1_at	XM_002298315 ^a	Rhomboid family protein	1.90	>5	POPTR_0001s24800
PtpAffx.204967.1.S1_at	XM_002313397	Rhomboid family protein	1.56	>2	POPTR_0009s03720
PtpAffx.32440.1.S1_at	XM_002298020 ^a	Rhomboid family protein	1.72	>10	POPTR_0001s08920
PtpAffx.130641.1.S1_s_at	XM_002314170 ^a	Kinesin motor family protein	1.52	>10	POPTR_0009s03110
PtpAffx.200613.1.S1_at	XM_002298181	Kinesin motor family protein	1.53	>5	POPTR_0001s18260
PtpAffx.147624.1.A1_at	XM_002310259	Kinesin motor family protein	1.59	>25	–
PtpAffx.57355.1.S1_at	XM_002299861	Kinesin motor protein-related	1.52	>2	–
PtpAffx.144831.1.S1_s_at	XM_002299432 ^a	ADL1 (dynamin-like protein);	1.70	>2	–
PtpAffx.210802.1.S1_at	XM_002318256	DRP3A (dynamin-related protein 3A)	1.22	>10	POPTR_0007s02960
PtpAffx.117056.1.S1_s_at	XM_002314165 ^a	TIP1;3 water channel	3.65	>10	–
PtpAffx.3989.1.S1_at	XM_002311110 ^a	TIP1;3 water channel	2.43	>1	–
PtpAffx.52659.1.A1_at	XM_002299857 ^a	TIP1;3 water channel	1.66	>5	–
PtpAffx.2848.1.S1_at	XM_002309090 ^a	PIP subfamily	–1.98	>10	–
PtpAffx.202247.1.S1_at	XM_002301360	CRF2 (cytokinin response factor 2)	1.12	<–1	None
PtpAffx.5552.2.S1_s_at	XM_002304642 ^a	Histidine kinase cytokinin receptor	–2.35	<–5	None
Ptp.811.1.A1_at	XM_002304642 ^a	Histidine kinase cytokinin receptor	–2.19	>1	–
PtpAffx.201634.1.S1_at	XM_002300706	CKX5 (cytokinin oxidase 5)	–1.28	<–10	POPTR_0002s03190
PtpAffx.218925.1.S1_at	XM_002332387	CKX6 (cytokinin oxidase/dehydrogenase 6);	1.19	>6	POPTR_0001s05830
Ptp.938.1.A1_s_at	XM_002309432	CKX7 (cytokinin oxidase 7);	–1.13	>2	None
PtpAffx.31331.2.A1_a_at	XM_002304758	Type-a response regulator (ARR9)	1.28	>2	None
PtpAffx.44007.2.A1_at	XM_002312733	Type-a response regulator	1.37	>100	None
PtpAffx.44007.3.S1_a_at	XM_002312663	Type-a response regulator	1.42	>1	None
PtpAffx.201936.1.S1_at	XM_002301034 ^a	PUP3 cytokinin transporter	–2.21	>1	POPTR_0002s09980
PtpAffx.205454.1.S1_s_at	XM_002307315	PUP2 cytokinin transporter	–1.18	>1	None
PtpAffx.39343.1.S1_at	XM_002302194	Type-a response regulator	1.26	>5	None

Table 1 continued

Probe	Genbank ID	Description	FC	EXP _{V/L}	Poplar V2.0 ID
PtpAffx.158523.1.S1_s_at	XM_002310744 ^a	Glycosyltransferase, CAZy family GT8	1.58	>10	None
PtpAffx.222470.1.S1_at	XM_002328075 ^a	ABA2 xanthoxin dehydrogenase	-1.94	<-10	POPTR_0004s21040
PtpAffx.6684.2.S1_s_at	XM_002328075 ^a	ABA2 xanthoxin dehydrogenase	-1.74	<-20	
PtpAffx.221010.1.S1_s_at	XM_002307113 ^a	ABA-responsive protein-related	-1.93	>10	POPTR_0005s09060
PtpAffx.205234.1.S1_s_at	XM_002333696 ^a	ABA-responsive protein-related	-1.82	>20	POPTR_0005s09050
PtpAffx.202059.1.S1_at	XM_002301149 ^a	CYP707A4; (+)-abscisic acid 8'-hydroxylase	1.75	>20	-
Ptp.2599.1.S1_s_at	XM_002300667 ^a	Tubulin, beta chain	2.59	>5	
Ptp.5472.1.S1_at	XM_002313977 ^a	Tubulin, beta chain	1.97	>25	
PtpAffx.135374.1.S1_at	XM_002298784	ATMAP65-1 microtubule binding	1.43	>25	POPTR_0001s36650
Ptp.7295.1.S1_at	XM_002307873	ATMAP70-5 microtubule binding	1.09	>5	POPTR_0006s01900
PtpAffx.1704.5.A1_at	-	TUB7, beta-tubulin 7	1.30	>25	POPTR_0001s27960
Ptp.5933.1.S1_x_at	XM_002298418	TUB3, beta-tubulin 3	1.40	>5	POPTR_0001s27960
Ptp.5651.1.S1_s_at	XM_002322573 ^a	TUB3, beta-tubulin 6	1.80	>2	-
Ptp.770.1.A1_s_at	XM_002316365 ^a	RABC2A, GTP binding	1.82	>10	-
PtpAffx.146219.1.S1_at	XM_002320185 ^a	GTPase activating protein	2.00	<-1	POPTR_0014s09940
PtpAffx.157389.1.S1_at	XM_002301394 ^a	Rac GTPase activating protein	1.96	>10	-
PtpAffx.211787.1.S1_s_at	XM_002321005 ^a	Rac GTPase activating protein,	1.87	>2	POPTR_0014s13090
Ptp.7759.1.S1_at	XM_002322494 ^a	Rho GDP-dissociation inhibitor	1.66	>2	-
Ptp.1990.1.S1_a_at	XM_002325552 ^a	ROP2, rho-related protein	1.90	>10	POPTR_0019s12210
PtpAffx.10764.1.S1_at	XM_002309059 ^a	ROPGEF7; Rho guanyl-nucleotide exchange	2.35	>20	POPTR_0006s09370
PtpAffx.213572.1.S1_at	XM_002323495 ^a	ROPGEF7; Rho guanyl-nucleotide exchange	1.71	>20	POPTR_0016s10130
Ptp.5677.1.S1_at	XM_002318658 ^a	Pectate lyase family protein	1.63	>10	-
Ptp.4652.1.S1_s_at	XM_002300033 ^a	Pectate lyase family protein	1.12	>5	POPTR_0001s35960
PtpAffx.210733.1.S1_at	XM_002318179 ^a	Pectinacetyltransferase, putative	2.00	>10	POPTR_0012s13090
PtpAffx.137964.1.S1_s_at	XM_002318883 ^a	Pectinacetyltransferase, putative	1.75	>100	POPTR_0013s00280
PtpAffx.42470.1.S1_s_at	XM_002329532 ^a	Clathrin adaptor, medium subunit	1.78	>1	-
PtpAffx.137956.1.S1_at	XM_002309487 ^a	Clathrin assembly protein-related	2.01	>1	-
Ptp.1826.1.S1_at	XM_002308250	Clathrin adaptor, small chain	1.54	<-1	POPTR_0006s15350
PtpAffx.6486.2.S1_a_at	XM_002318496	Clathrin adaptor, small chain	1.39	>1	POPTR_0014s07500
PtpAffx.78955.1.S1_at	XM_002302304	Clathrin adaptor, medium subunit	1.37	>1	POPTR_0002s10530
PtpAffx.210842.1.S1_at	XM_002318903	Clathrin adaptor, medium subunit	1.39	>2	POPTR_0013s00780
PtpAffx.1066.10.S1_a_at	XM_002318255	Clathrin adaptor, medium subunit	1.57	>1	POPTR_0012s14780
PtpAffx.99026.1.S1_at	XM_002298450	Clathrin heavy chain	1.30	>25	POPTR_0001s28540
PtpAffx.162111.1.S1_at	XM_002298450	Clathrin heavy chain	1.40	>2	POPTR_0009s07740

FC is the fold change of expression in CO₂ fumigated trees verse controls. EXP_{V/L} is the range of expression ratio of VCZ to leaf. In this study, we defined a gene to be VCZ-specific if EXP_{V/L} >5 and leaf-specific if EXP_{V/L} <-5. The range is defined as follows: >1: FC = 1-2, >2: FC = 2-5, >5: FC = 5-10, >10: FC = 10-20, >25: FC = 25-100, >100: FC > 100

^a The identified DEGs in VCZ. Other genes are listed for comparison

XM_002312663, XM_002302194, XM_002304758 and XM_002312733, which encode a cytokinin-inducible type-a response negative regulator (To et al. 2007), were up-regulated 41.7, 26.4, 28.2 and 37.4 %, respectively. These type-a response regulators suppress the cytokinin signaling (Hirose et al. 2007) and can thus be a part of mechanism that wears down the increased cytokinin signaling.

Three genes, XM_002314165, XM_002311110, and XM_002299857, of the aquaporin TIP family protein, were

up-regulated significantly in VCZ in response to elevated [CO₂]. TIP family proteins function on the vacuolar membrane (Barkla et al. 1999; Maeshima 2001). We theorize that this increase facilitated expansion of the newly formed primary xylem cells. However, the genes encoding plasma membrane intrinsic protein (PIP) in VCZ were down-regulated. The changes of these genes suggest an alternation of inter- and intracellular communication through membrane transport properties of aquaporins.

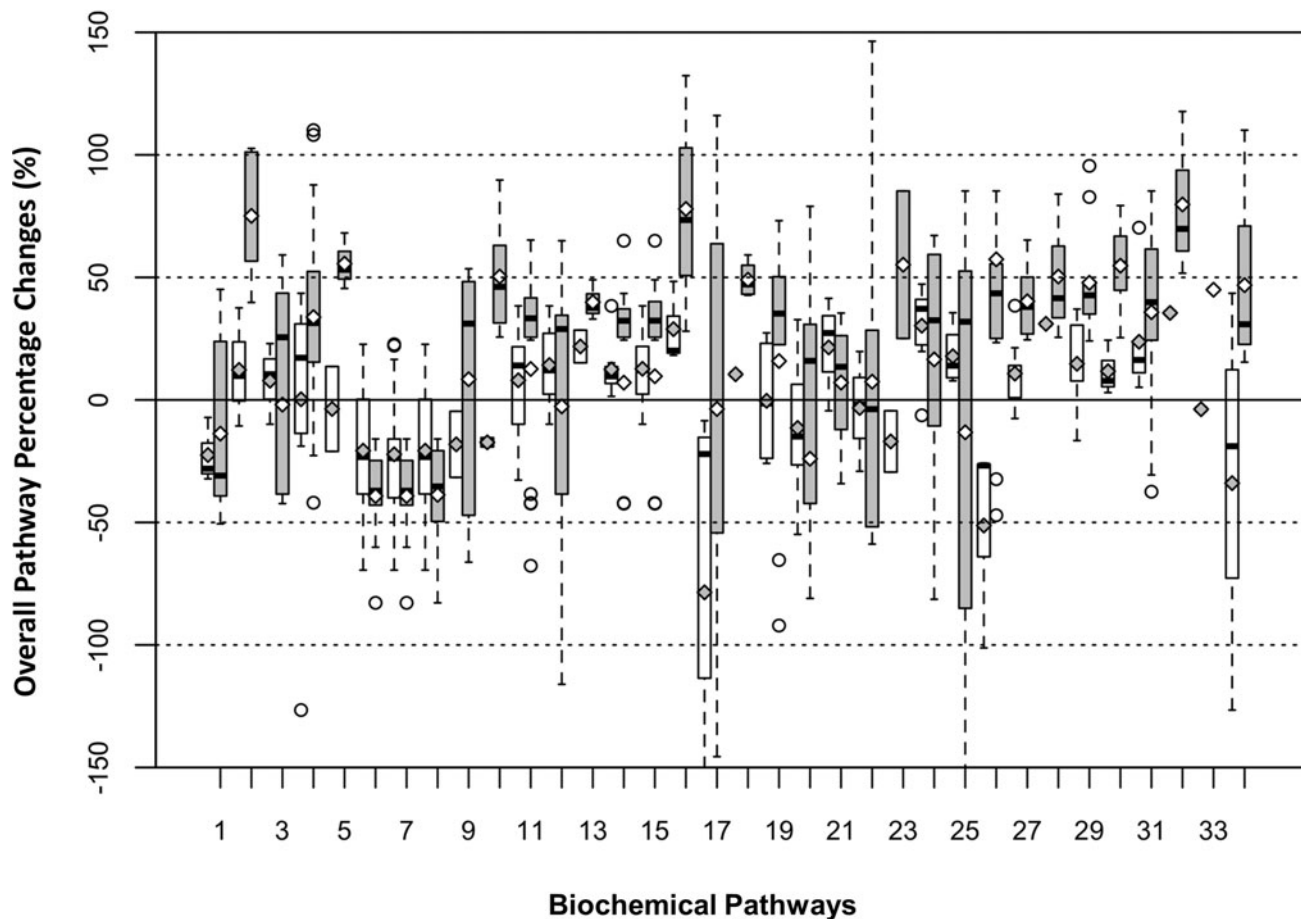
Differentially Altered pathways in VCZ and Leaves in Response to Elevated [CO₂]

Fig. 2 Boxplot of the overall percentage change of each pathway in response to elevated [CO₂]. The median and the average percentage change of each pathway are represented by the *black line* and *diamond* inside the *bar*, respectively. The *white* and *gray bars* represent leaves and the VCZ, respectively. Pathway names corresponding to the numbers shown in the *x-axis* labels listed above, and the numbers following L or VCZ shown in the parentheses at the end of each pathway name are the pathway gene numbers used to calculate the overall pathway percentage change in leaves and VCZ. The genes with an expression level ($<2^5 = 32$) in both control and treatment were considered unexpressed and were excluded from pathway analysis given the maximal expression level is more than 9 magnitudes more ($2^{14.21} = 18,951$). 1, Abscisic acid biosynthesis (L2, VCZ5); 2, acetyl-CoA biosynthesis (from citrate) (L3, VCZ6); 3, Calvin-Benson-Bassham cycle (L3, VCZ14); 4, cellulose biosynthesis (L9, VCZ13); 5, chorismate biosynthesis I (L2, VCZ3); 6, cytokinins 7-*N*-glucoside biosynthesis (L12, VCZ9); 7, cytokinins 9-*N*-glucoside biosynthesis (L13, VCZ9); 8, cytokinins-*O*-glucoside biosynthesis (L12, VCZ18); 9, GDP-glucose biosynthesis (L2, VCZ6); 10, GDP-

mannose biosynthesis (L2, VCZ6); 11, gluconeogenesis I (L7, VCZ21); 12, glycolysis I (L2, VCZ17); 13, glycolysis II (L8, VCZ3); 14, glycolysis IV (plant cytosol) (L7, VCZ15); 15, glycolysis V (L7, VCZ16); 16, homogalacturonan biosynthesis (L3, VCZ3); 17, homogalacturonan degradation (L13, VCZ12); 18, pentose phosphate pathway (non-oxidative branch) (L1, VCZ4); 19, pentose phosphate pathway (oxidative branch) (L4, VCZ9); 20, phenylpropanoid biosynthesis (L5, VCZ9); 21, phenylpropanoid biosynthesis, initial reactions (L3, VCZ4); 22, photorespiration (L4, VCZ10); 23, starch biosynthesis (L2, VCZ2); 24, starch degradation (L8, VCZ7); 25, sucrose biosynthesis (L4, VCZ7); 26, sucrose degradation III (L3, VCZ13); 27 TCA cycle variation III (plant) (L9, VCZ7); 28, UDP-D-galacturonate biosynthesis I (from UDP-D-glucuronate) (3) (L1, VCZ3); 29 UDP-D-xylose biosynthesis (25) (L6, VCZ11); 30, UDP-galactose biosynthesis (salvage pathway from galactose using UDP-glucose) (L3, VCZ7); 31, UDP-glucose biosynthesis (from glucose 6-phosphate) (L6, VCZ14); 32, UDP-L-arabinose biosynthesis I (from UDP-xylose) (L1, VCZ3); 33, UDP-L-rhamnose biosynthesis (L1, VCZ1); 34, xylan biosynthesis (L3, VCZ4)

Overall pathway expression changes

The existence of multiple enzymes that catalyze the same step of a biochemical reaction in a given pathway makes the evaluation of the on/off status by examining only the statistically DEGs quite inadequate. In the present study,

we also calculated an overall pathway change in expression of each pathway and used this to identify the pathways in which genes were collectively up/down-regulated (Fig. 2).

The overall average expression of Calvin cycle pathway genes in leaves increased 7.8 % in response to elevated [CO₂] but almost has no increase (−2 %) occurred for these

genes in the VCZ. Several genes in this pathway, including fructose-1,6-bisphosphatase (FBPase) transketolase, and aldolase that have been linked to growth in tobacco (Lefebvre et al. 2005; Tamoi et al. 2006; Uematsu et al. 2012), increased. The average expression of several down-stream pathways that assimilate the products of Calvin cycle were all up-regulated. Interested users can find more detailed information for these leaf responses in Supplemental File 1.

Acetyl-CoA is a central metabolite in many aspects of plant metabolism. Its biosynthesis pathway is a linked pathway of Glycolysis I, II, and IV, and the super pathway of TCA cycle, cytokinin, and gibberellins A12 biosynthesis. The overall average gene expression of acetyl-CoA biosynthesis from citrate was enhanced 75.1 % in VCZ under elevated [CO₂] (Fig. 2). This enhancement of acetyl-CoA biosynthesis pathway genes possibly arose to fulfill the need for generation of energy and gibberellins to promote stem elongation as cytokinins are assumed to be synthesized mainly in root cap columella (Aloni et al. 2005; Ghanem et al. 2011). The overall average expression of TCA cycle variation V (plant) increased 40.2 % in the VCZ, as compared to 10.3 % in leaves. Concomitant with this enhancement of acetyl-CoA biosynthesis, an average decrease of 39 % of all genes involved in three cytokinin glucoside biosynthesis pathways was noted under elevated [CO₂]. These pathways convert active cytokinins into inactive forms, suggesting a relative increase in the active forms of cytokinins in the VCZ. The abscisic acid (ABA) biosynthesis pathway decreased 13.8 % in VCZ and 22.5 % in leaves in response to elevated [CO₂] (Fig. 2), suggesting that various hormones were coordinated to enhance cambial growth.

The overall average expression of cellulose biosynthesis pathway increased 33.7 % in VCZ and 0.2 % in leaves, which reflects more intensive cell wall biosynthesis in VCZ. In addition, expression of genes for UDP-D-galacturonate biosynthesis I (from UDP-D-glucuronate), UDP-D-xylose biosynthesis, UDP-galactose biosynthesis (salvage pathway from galactose using UDP-glucose), UDP-glucose biosynthesis (from glucose 6-phosphate), UDP-L-arabinose biosynthesis I (from UDP-xylose), UDP-L-rhamnose biosynthesis, and xylan biosynthesis increased 50.3, 47.8, 54.8, 35.8, 79.7, 36.5, and 46.8 %, respectively in the VCZ, but changed by 31, 14.7, 11.7, 23.7, -5.7, -3.8, and -33.9 %, respectively, in leaves (Fig. 2). This suggests a significant boost in hemicellulose and pectin biosynthesis in the VCZ. As to lignin biosynthesis, the expression of three genes involved in the phenylpropanoid biosynthesis initial reactions increased by 7 % in VCZ and 21.4 % in the leaves. However, the overall average expression of phenylpropanoid biosynthesis decreased 24 % in VCZ and 11.4 % in leaves (Fig. 2). The lignin pathway was mainly regulated at 4-coumarate-

coa ligase (4LC) 4CL, and caffeate O-methyltransferase (OMT1). This is evidenced by the fact that three genes, XM_002327918, XM_002325779, and XM_002297663 encoding 4CL genes were down-regulated 286, 42 and 2 %, respectively in VCZ as the other gene, XM_002302640 encoding OMT1 decreased 81 % in VCZ.

Protein domain enrichment (PDE) analysis

Protein domain enrichment analysis can reveal which gene families are impacted by elevated [CO₂]. We performed PDE analysis of the DEGs in VCZ and displayed the expression patterns of four types of functional groups in Table 2, each representing a biological theme. To make the enriched domains between leaves and VCZ comparable, the enriched protein domains of leaves shown in Table 2 were derived from the top 1,961 genes of DEG list of leaves (rather than from 542 DEGs of leaves only). Group I contains those domains whose carriers generally had an increased average expression in VCZ and a decreased average expression in leaves. In Group II, three genes encoding auxin efflux carrier domain were down-regulated 77 % in VCZ, as compared to 17 % increase in leaves. There are seven down-regulated genes containing Aux/IAA domain in VCZ, which acts as repressors of auxin-induced gene expression, possibly through modulating the activity of DNA-binding auxin response factors (Tiwari et al. 2004; Tiwari et al. 2001). Coordinately, five genes encoding GH3 auxin-responsive promoter and functioning in conjugating auxin, decreased 128 % on average in VCZ, suggesting elevated [CO₂] can potentially increase auxin activity in VCZ. In Group III, six genes encoding water channel protein increased more than twofold in VCZ while some genes encoding water channel decreased in leaves nearly twofold. In Group IV, genes with domains that are known to be involved in cellulose biosynthesis, hemicellulose, and pectin biosynthesis increased more in VCZ than in leaves except that two domains, sucrose-6F-phosphate phosphohydrolase, and sucrose phosphate synthase, involved in sucrose biosynthesis decreased in VCZ but not in leaves.

Gene ontology (GO) term enrichment analysis

We performed GO term enrichment analysis on all DEGs from VCZ and found the cell wall organization and biogenesis associated biological processes were significantly enriched. Also enriched in VCZ were nucleoside metabolic processes, pigmentation processes, and transmembrane receptor protein tyrosine kinase signaling pathway. Interested readers can find more detailed information in Supplemental file 1.

Table 2 The protein domains enriched in the gene list of differentially expressed genes

Tissue	InterPro	Description	Gene num	EF	P-value	FC_AVG
Group I						
VCZ	IPR004367	Cyclin, C-terminal	3	1.40	0.1672048	1.18
Leaves	IPR004367	Cyclin, C-terminal	1	-2.12	0.6324380	-1.03
VCZ	IPR015451	Cyclin D	2	1.15	0.2140380	1.48
Leaves	IPR015451	Cyclin D	1	1.09	0.2305270	-1.03
VCZ	IPR013922	Cyclin-related 2	2	5.78	0.0041401	1.76
Leaves	IPR013922	Cyclin-related 2	1	2.75	0.0490771	1.68
VCZ	IPR016098	Cyclase-associated protein CAP	1	9.62	0.0035113	1.79
VCZ	IPR002963	Expansin	2	1.65	0.1199281	1.48
Leaves	IPR002963	Expansin	4	3.92	0.0015096	-1.51
VCZ	IPR007118	Expansin/Lol pI	5	3.92	0.0034707	1.81
Leaves	IPR007118	Expansin/Lol pI	5	4.47	0.0001407	-1.42
VCZ	IPR007112	Expansin 45, endoglucanase-like	6	3.15	0.0027936	1.75
Leaves	IPR007112	Expansin 45, endoglucanase-like	6	3.99	0.0001536	-1.34
Group II						
VCZ	IPR004776	Auxin efflux carrier	3	3.01	0.0171090	-1.77
Leaves	IPR004776	Auxin efflux carrier	3	2.36	0.0371110	1.17
VCZ	IPR003311	AUX/IAA protein	7	3.0	0.0024230	-2.70
Leaves	IPR003311	AUX/IAA protein	3	1.71	0.0971630	-1.66
VCZ	IPR003311	Aux/IAA-ARF-dimerisation	6	3.39	0.0017959	-2.02
Leaves	IPR011525	Aux/IAA-ARF-dimerisation	3	0.94	0.3908440	-1.66
VCZ	IPR004993	GH3 auxin-responsive promoter	5	7.22	4.35E-05	-2.28
Leaves	IPR004993	GH3 auxin-responsive promoter	1	1.37	0.1637392	1.11
Leaves	IPR015345	Cytokinin dehydrogenase I	2	4.58	0.0082474	-1.55
Group III						
VCZ	IPR012269	Aquaporin	6	2.75	0.0060042	2.05
Leaves	IPR012269	Aquaporin	4	1.74	0.0791068	-1.70
VCZ	IPR000425	Major intrinsic protein (water channel)	6	1.86	0.0426369	2.05
Leaves	IPR000425	Major intrinsic protein (water channel)	10	2.95	0.0005671	-2.10
Group IV						
VCZ	IPR005150	Cellulose synthase	2	0.93	0.3636904	1.93
Leaves	IPR005150	Cellulose synthase	6	2.82	0.0071798	1.27
VCZ	IPR016461	O-methyltransferase, COMT	2	1.75	0.1050379	-2.68
Leaves	IPR016461	O-methyltransferase, COMT	2	1.66	0.1174360	-1.35
VCZ	IPR006151	Quinate/shikimates5-dehydrogenas	2	1.31	0.1759511	-2.46
VCZ	IPR010713	Xyloglucan endo-transglycosylase, C-terminal	5	2.83	0.0081207	1.45
Leaf	IPR010713	Xyloglucan endo-transglycosylase, C-terminal	8	4.85	1.30E-05	-2.40
VCZ	IPR014027	UDP-glucose/GDP-mannose dehydrogenase	5	10.5	1.92E-05	1.95
VCZ	IPR002213	UDP-glucuronosyl/UDP-glucosyltransferase	2	3.39	0.0195882	2.28
Leaves	IPR002213	UDP-glucuronosyl/UDP-glucosyltransferase	1	1.61	0.1256750	1.54
VCZ	IPR005886	UDP-glucoses4-epimerase	1	1.81	0.1043882	2.17
VCZ	IPR017761	Laccase	9	5.77	2.53E-06	1.22
Leaves	IPR017761	Laccase	2	1.22	0.224673	1.11
VCZ	IPR004963	Pectinacetylase	2	2.22	0.0596068	1.88
Leaves	IPR004963	Pectinacetylase	2	2.11	0.0672154	-2.19
VCZ	IPR006380	Sucrose-6F-phosphate phosphohydrolase	2	3.61	0.0165502	-2.63
Leaves	IPR006380	Sucrose-6F-phosphate phosphohydrolase	1	1.72	0.1135182	1.65
VCZ	IPR012819	Sucrose phosphate synthase, plant	2	7.22	0.0020352	-2.63

Table 2 continued

Tissue	InterPro	Description	Gene num	EF	P-value	FC_AVG
Leaves	IPR012819	Sucrose phosphate synthase, plant	1	3.43	0.0320401	1.65
VCZ	IPR005829	Sugars transporter, conserved site	4	0.92	0.432882	3.18
Leaves	IPR005829	Sugars transporter, conserved site	6	1.09	0.310526	-1.06
VCZ	IPR017853	Glycoside hydrolase, catalytic score	20	1.89	0.002459	2.99
Leaves	IPR017853	Glycoside hydrolase, catalytic score	40	2.97	3.19E-10	1.14

EF enrichment factor in the background of all genomic genes, FC_AVG averaged fold change

Discussion

Why do trees grow faster under elevated [CO₂]?

The results described in this study were from genome-wide microarray and thus may provide a more holistic picture of why elevated [CO₂] can enhance tree growth. In our leaf samples, the genes in Calvin cycle were expressed at a 7.8 % higher rate under elevated [CO₂] than in the control, while the genes involved in photorespiration were reduced 3.3 %. The linked pathways including gluconeogenesis, glycolysis I, glycolysis I (cytosolic), glycolysis IV (plant cytosol), glycolysis V, pentose phosphate pathway (non-oxidative branch) that consume the Calvin cycle products increased 8, 14.2, 21.8, 2.4, 21.8 and 10.5 %, respectively. The assimilated carbon can provide a stimulus for many biological processes through various mechanisms. Although most of these mechanisms remain elusive, work with algae indicated that elevated [CO₂] can drive gene expression through activation of enhancers (Fukuzawa and Yamano 2005). In addition, it is well-known that newly synthesized carbohydrates can serve as signaling molecules to activate the expression of a large number of genes and change source/sink relationships (Avonce et al. 2005; Meyer et al. 2007; Nielsen et al. 2004; Thomas and Rodriguez 1994).

In VCZ, the enhancement of genes involved in carbohydrate metabolism is accompanied by the up-regulation of genes encoding cyclins, expansins, auxin amido synthetases, auxin influx carriers, ABA hydroxylase, glycosyl hydrolases, and Ras signaling proteins, and the down-regulation of ABA biosynthesis, and cytokinins degradation genes in the VCZ of CO₂ treated trees. Since previous work clearly shows that cytokinins are the determinants of cambial activity (Nieminen et al. 2008), the ~39 % decrease in expression of the pathway genes responsible for cytokinin glucosylation, and the 28 and 13 % decrease in the expression of two genes, XM_002300706 and XM_002309432 encoding cytokinin oxidase, could result in increased levels of active cytokinins in the VCZ of CO₂ fumigated trees. Additionally, the increased expression of multiple genes encoding clathrin, dynamin, tubule, kinesin

and cyclins suggests the augmentation of activities of many cellular processes that include vesicular transport, mitosis, and cytokinesis in the VCZ in response to elevated [CO₂].

Domain analysis shows genes encoding aquaporins and major intrinsic protein (water channel) significantly increased 74–195 % in VCZ under elevated [CO₂], indicating elevated [CO₂] can enhance water conductivity in developing wood. We assume this was to fulfill a need for cell expansion. We do not have sufficient data to explain why six genes encoding aquaporin and 10 genes encoding major intrinsic protein were on average down-regulated in leaves (Table 2) though we speculate this phenomenon has something to do with temporal drought, or water use efficiency. In previous study, Gupta et al. (2005) reported two genes encoding aquaporin PIP 2a were down-regulated 18–58 % in leaves in response elevated [CO₂]. We also observed that two aquaporin genes encoding PIP 2b and one PIP subfamily gene in VCZ under elevated [CO₂] were down-regulated 27–98 % in leaves (Table 1). Generally, it is assumed that elevated CO₂ causes stomatal closure, and consequently, increases the water use efficiency (Conley et al. 2001; Li et al. 2008). Anyway, our finding of the up-regulation of TIP genes and down-regulation of PIP genes in VCZ upon CO₂ fumigation can serve as a starting point for future research for exploitation of roles of aquaporin gene family in CO₂ fumigated trees.

Lignocellulosic biosynthesis

The overall pathway of cellulose biosynthesis increased 33.7 % in VCZ and 0.2 % in leaves while the lignin biosynthesis pathway decreased 24 % in VCZ and 11.4 % in leaves. Most genes except three 4CL and one OMT1 in phenylpropanoid biosynthesis pathways were up-regulated. Since 4CL genes catalyze the 3rd step of phenylpropanoid biosynthesis pathway, beyond which, the pathway bifurcates into multiple branches, the down-regulation of three 4CL genes can constitute a rate limiting control on lignin biosynthesis. In addition, the expression of genes for ferulate and sinapate biosynthesis pathways that consume sinapaldehyde increased 14 % in VCZ and decreased 3.4 % in leaves. This piece of evidence is consistent with the idea

that lignin synthesis is down-regulated in VCZ in response to elevated $[\text{CO}_2]$.

As we indicated earlier, down-regulation of lignin biosynthesis is important for maintaining the growth phase of cells in the VCZ. However, Druart et al. (2006) found lignin biosynthesis was stimulated by growth under elevated $[\text{CO}_2]$. This inconsistency may be due in part to differences between our study and theirs in location of sampled materials and harvest time. They harvested stem materials from 15–25 cm below the apical meristems of 3-year-old coppice trees. In addition, they harvested their materials in November, as the growing season was ending and new growth often is declining, and intensive lignification is more likely (Casler et al. 2002; Macdonald 1986). We harvested our experimental materials during a period of active growth in July from the VCZ within the 1.5–2.5 meter region from ground of 12-year-old trees. In addition, Druart et al. (2006) used 800 and 1,200 $\mu\text{mol mol}^{-1}$ $[\text{CO}_2]$ to treat plants, a much higher level than we used. All of these factors could create differences that are not yet clearly understood.

Noncellulosic polysaccharide synthesis in cell wall is enhanced under elevated $[\text{CO}_2]$

We have shown that the overall gene expression of several pathways, including UDP-D-galacturonate biosynthesis I (from UDP-D-glucuronate), UDP-D-xylose biosynthesis, UDP-galactose biosynthesis (salvage pathway from galactose using UDP-glucose), UDP-glucose biosynthesis (from glucose 6-phosphate), UDP-L-arabinose biosynthesis I (from UDP-xylose), and UDP-L-rhamnose biosynthesis and xylan biosynthesis increased by at least 35 % in VCZ when compared to controls, and at least 19 % more increase as compared to the increase in leaves (Fig. 2). In agreement with these changes, the average expression of all 29 genes encoding glycosyltransferase CAZy GT 8 family proteins increased 34.7 % in the VCZ of CO_2 treated trees. The proteins of this family are localized in the Golgi apparatus, the site of synthesis of noncellulosic polysaccharides (Herrero et al. 2004). This family is implicated in pectic polysaccharide biosynthesis (Bootten et al. 2004), which possibly define the extensibility of the cell wall and the incorporation of new polymers into the expanding cell wall.

All evidence we have shown here supports a significant increase in pectin and hemicellulose biosynthesis in response to growth under elevated $[\text{CO}_2]$ (Fig. 2). We speculate that these increases can contribute to cell division and expansion by supporting the formation of new wall material when cells divide or grow during rapid cambial growth. Since pectin and hemicellulose biosynthesis are closely linked to cellulose biosynthesis, the significant biosynthesis of pectin and hemicellulose can counterbalance cellulose biosynthesis. This may be a characteristic of the

VCZ, where proper cell wall rigidity and extensibility need to be maintained in order to fulfill maximal growth potential. We observed a clearly coordinated increase among these three pathways in response to growth under elevated $[\text{CO}_2]$.

Possible mechanisms underpinning cambial growth

Our analyses suggest the presence of multiple mechanisms that are responsible for the increased cambial growth in aspen trees under elevated $[\text{CO}_2]$. These include the up-regulation of the genes encoding auxin influx carriers, expansin gene family, and TIP aquaporin TIP family, and the down-regulation of the genes involved in ABA biosynthesis, cytokinin and auxin inactivation. In addition, the up- and down-regulation of f-box gene family, and genes involved in Ras-signaling pathway may play an even more important role in radial growth in response to elevated $[\text{CO}_2]$. This is because the changes of genes in the Ras-signaling pathway are not only differentially expressed in VCZ but also more VCZ-specific (Table 1). Ras proteins are small GTPases that regulate cell growth, proliferation, and differentiation (Ma 2007; Smith 1999; Yang 2002). They are known to control the mouse stem cell cycle via PI3K signaling pathways (Takahashi et al. 2003). In yeast, another signaling pathway, called ‘the target of rapamycin (TOR)’, merges with the PI3K signaling pathway to control cell growth (Deprost et al. 2007; Nakashima et al. 2008; Zaragoza et al. 1998). Evidence shows that the TOR pathway in plants determines organ sizes (Deprost et al. 2007; Krizek 2009), whereas the PI3K signaling pathway controls the G1/S transition in stem cells by shortening the cell cycle from 24 to 10 h (Liu et al. 2006). In Arabidopsis, the loss-of-function PI3K mutant causes severe defects in growth (Welters et al. 1994). The up-regulation of five xylem-specific genes involved in Ras signal transduction suggests a thriving of Ras signaling during cambial growth.

Conclusion

The transcriptome profiles of aspen trees grown under elevated $[\text{CO}_2]$ for 12 years were dissected and contrasted with control trees. Elevated $[\text{CO}_2]$ enhanced expression of the genes catalyzing most of the reactions of carbon fixation (Calvin cycle) in leaves, which presumably would lead to the biosynthesis of more metabolites. Some specific metabolites could serve as signaling molecules to cause changes in gene expression in the VCZ. These changes could include, but would not be limited to, the genes involved in hormone metabolism, polysaccharide transport, cell division, cell wall loosening, and cell wall formation. Although expression of these genes changed by small magnitudes, collectively, increased expression changes

could augment cambial and xylem cell division and expansion, thereby leading to significantly increased biomass production in perennial trees. Among multiple molecular mechanisms identified, it appears that hormone metabolism, cell division and expansion, as well as Ras signaling pathway were more conspicuous in the data we generated. Certainly, more studies on spatiotemporal samples from other tissues and at various stages of the growing season will be needed to learn the whole story of underlying molecular events inside of the CO₂ fumigated trees.

Materials and methods

Aspen FACE experiment

The Aspen FACE experiment site was located near Rhineland, WI, USA (89.5°W, 45.7°N). The experiment operated from 1998 through 2009 and used a full factorial design consisting of twelve 30-m diameter rings, three of which were allocated to each of four treatments: control (ambient CO₂ of $\approx 360 \mu\text{mol mol}^{-1}$, ambient O₃ of $\approx 36 \text{ nmol mol}^{-1}$); elevated [CO₂] (560 $\mu\text{mol mol}^{-1}$); elevated O₃ (1.5 \times ambient); and elevated [CO₂] plus elevated O₃ (Dickson et al. 2000). Only trees from the control and elevated [CO₂] treatments from two rings were used in this study. During the portion of 2009 prior to the date when plant materials for this study were obtained, control rings had an average [CO₂] of 380 $\mu\text{mol mol}^{-1}$ and the elevated [CO₂] treatment had average [CO₂] of 560 $\mu\text{mol mol}^{-1}$. The elevated [CO₂] treatment was applied during daylight hours from bud break in the spring until leaf senescence in the fall, a period that averages 146 day per year (King et al. 2005). The twelve 30-m diameter rings were fumigated using a FACE technology system that combines a gas monitoring system with a delivery system of blowers and vertical pipes placed around the plot perimeter (Dickson et al. 2000). The 1-min average CO₂ concentrations were within 20 % of the target. The precipitation at the FACE site from 2007 to 2009 is shown in Table 3. Compared to other years, there was a temporal water shortage in June and July of 2009.

Table 3 The precipitation at the FACE site from 2007 to 2009

Month	2007 (mm)	2008 (mm)	2009 (mm)
Mar	61.7	22.1	43.2
Apr	31.2	83.5	80.1
May	NA	58.9	75.4
Jun	82.3	45.2	36.8
Jul	113.4	66.3	30.0

Plant materials

The aspen trees in the experiment were planted from cuttings in 1997 at a 1 m \times 1 m spacing. Five trembling aspen genotypes of differing CO₂ and O₃ responsiveness were used in the main experiment (Dickson et al. 2000; Kubiske et al. 2007). On July 28, 2009, leaves and VCZ tissues were harvested from two aspen clones, 42E and 271 that have similar positive responses under elevated [CO₂] and show no significant difference in height and diameter (Isebrand et al. 2001; Kubiske et al. 2007). Eight aspen trees: 2 clones (42E and 271) \times 2 treatments (ambient control and elevated [CO₂] \times 2 replicates (8 trees in total) were initially harvested (Fig. 1). For each tree, we harvested two tissue types: leaves and VCZ. Leaf tissues were collected from 1/4 height of canopy from the highest apical meristem when fumigation was in full operation, and VCZ samples were harvested by gently scratching a thin layer of $\sim 10 \mu\text{m}$ around the vascular cambium at approximately 1.5–2.5 m aboveground, based on an earlier description of morphological sections (Du et al. 2006). The 8 samples for each type of tissues (16 samples in total) were harvested and then immediately flash-frozen in liquid nitrogen and subsequently stored in $-80 \text{ }^\circ\text{C}$ freezers. Size differences between the sampled control and elevated [CO₂] fumigated trees (Fig. 1) were consistent with the long-term measured growth increases reported for elevated [CO₂] earlier in the experiment (King et al. 2005, Kubiske et al. 2007).

RNA isolation and preparation

Total RNA was isolated with a modified Qiagen RNeasy Mini kit protocol (Qiagen: <http://www.qiagen.com/>) as we described earlier (Busov et al. 2003). Approximately 0.2 g of VCZ or mature leaf tissue was ground in liquid nitrogen, and then 1 ml of lysis buffer (addition of 0.01 g of polyvinylpyrrolidone to the buffer before using) was added to the fine powder. After homogenizing 45 s using a Polytron, 400 μl of 5 M K-acetate was added and the slurry was incubated on ice for 15 min. The extracts were then centrifuged for 10 min at 4 $^\circ\text{C}$ at 16,000 \times g. The supernatant was mixed with 700 μl of 100 % (w/v) ethanol and this was applied to the RNeasy mini column. The remaining steps followed the kit procedures precisely. Prior to labeling with fluorescent dye, RNA quality was assessed with an Agilent Bioanalyzer (Agilent Technologies, USA).

Poplar arrays and hybridization

GeneChip[®] Poplar Genome Arrays were obtained from Affymetrix Inc. (Santa Clara, CA, USA). This platform is based on NCBI Genbank sequences of various poplar

species that were available as of April 26, 2005 and the earlier released gene models from the *Populus trichocarpa* genome sequences (Tuskan et al. 2006). Each array contains about 61,413 oligonucleotide probe sets representing more than 61,252 transcripts from multiple poplar species, with several internal control genes for normalization. During material storage and transfer, we lost one treated sample and one control sample of clone 271 from leaves. As a result, we had 14 RNA samples being hybridized. They are: 8 RNA samples from VCZ, 2 clones (42E and 271) \times 2 treatments (Control and CO₂ treatment) \times 2 replicates (trees); and 6 RNA samples from leaves, 2 treatments \times 2 replicates for Clone 42E, and 2 treatment \times 1 replicate for Clone 271. Prior to labeling, RNA quality was assessed by Agilent Bioanalyzer (Agilent Technologies, USA) and 0.2 μ g of total RNA was used to prepare biotinylated complementary RNA (cRNA) by following Affymetrix's GeneChip[®] 3' IVT Expression Labeling Assay protocol. The hybridization, and imaging procedures were performed according to Affymetrix's GeneChip[®] Expression Analysis Technical Manual using GCOS software at the at the Integrated Genomics Facility, Kansas State University, Manhattan, KS 66506, following the recommended procedure from Affymetrix (Affymetrix.com).

Data quality control and preparation

We used box-plots to check the mean and approximate distribution of each data set (chip). The Studentized deleted residual for each chip was then compared against a t-distribution (Persson et al. 2005a; Trivedi et al. 2005). Significant deviation from *t* distribution of Studentized deleted residuals for each data set indicates that the quality of the data set is problematic and provides a criterion for excluding that data set. Calculation of Kolmogorov–Smirnov for each sample was followed with an empirical cut-off of 0.15 as described in our earlier publication (Persson et al. 2005b) to identify quality chips. We normalized the data with robust multichip average (RMA) algorithm (Irizarry et al. 2003).

Identification of differentially expressed genes

Rank product (RP) (Breitling et al. 2004) was implemented to the data sets resulting from RMA normalization to identify DEGs. All genes were first sorted by p-values and then corrected with Benjamini and Hochberg False Discovery Rate (Benjamini and Hochberg 1995). The genelist was sorted again by the corrected p-values, and those genes with corrected p-values smaller than 0.05 were treated as DEGs.

Homology gene mapping and pathway analysis

The BLASTN program contained in the Basic Local Alignment Search Tool (BLAST) (Altschul et al. 1990) was used to identify the homologous genes between Affymetrix target sequences and gene model sequences of V2.0 releases for *Populus trichocarpa* (www.phytozome.org). Cut-off criteria applied included an E-value of 10 and a match of at least 90 % to the shorter sequence of either query or database. If more than one gene was matched, the one with maximal match was regarded as the homolog in the *Populus trichocarpa* genome. Due to the lack of annotation for most *Populus* genes, we also took advantage of the annotation for Arabidopsis genes to interpret some results generated from expression data analysis. BLASTX was employed to identify Arabidopsis homologous genes between Affymetrix target sequences and Arabidopsis protein sequences. The Arabidopsis protein sequences of TAIR10 release were downloaded from <http://www.arabidopsis.org/>. The criteria for selecting orthologs were similar to the criteria for BLASTN, except that the criterion for percent match was at least 40 %. Only the best-matched gene was considered to be the homologous gene. The pathway genes were identified by mapping all genes to the PoplarCyc and Aracyc pathway data stored in Plant Metabolic Network (<http://plantcyc.org/>), and the percentage change of each gene was calculated based on the averaged control and treatment. The overall change of each pathway was calculated by averaging the increased percentage portion of each gene.

Protein domain enrichment analysis

Protein domains were analyzed with InterproScan (Zdobnov and Apweiler 2001). We downloaded InterproScan and associated databases and installed them to our Linux server so that we could perform the standalone analysis to identify protein domains of all target sequences provided by Affymetrix. The enrichment of each domain in the DEG list was analyzed in the background of all genomic genes, and two parameters were introduced to show the enrichment of each domain: (1) Enrichment factor, $EF = k/(mn/N)$; and (2) the E_{score} , which is the hypergeometric probability of this domain calculated using the following formula:

$$E_{score} = 1 - \sum_{i=0}^{k-1} \frac{\binom{M}{i} \binom{N-M}{n-i}}{\binom{N}{i}}$$

where N is the total number of protein domains for all protein sequences in the genome, n is the total number for a specific domain in the genome, M is the number of all

protein domains in the DEG list, and x is the number of a specific domain present in the DEGs list. The E_score represents the upper boundary of geometric probability. In order to compare the VCZ with leaves, the same number of genes as the DEGs in VCZ were cut-off from the sorted gene (by p values) of leaves and used for PDE analysis.

Gene ontology term enrichment analysis

The DEGs from VCZ were used for gene ontology analysis using AmiGO's Term Enrichment tool (<http://amigo.geneontology.org/>). This tool uses Perl module GO:TermFinder available at CPAN (<http://search.cpan.org/>) to identify the enriched GO terms associated with a DEG list via hypergeometric probability as we described for protein domain above. We set the threshold p -value = 0.01 as the significance level. Similar to PED analysis, the same number of genes as the DEGs in VCZ were cut-off from the sorted gene (by p values) of leaves and used for gene ontology term enrichment analysis.

References

- Aloni R, Langhans M, Aloni E, Dreieicher E, Ullrich CI (2005) Root-synthesized cytokinin in Arabidopsis is distributed in the shoot by the transpiration stream. *J Exp Bot* 56:1535–1544
- Altschul SF, Gish W, Miller W, Myers EW, Lipman DJ (1990) Basic local alignment search tool. *J Mol Biol* 215:403–410
- Angelis PD, Chigwerewe KS, Scarascia Mugnozza GE (2004) Litter quality and decomposition in a CO₂-enriched Mediterranean forest ecosystem. *Plant Soil* 224:31–41
- Avonce N, Leyman B, Thevelein J, Iturriaga G (2005) Trehalose metabolism and glucose sensing in plants. *Biochem Soc Trans* 33:276–279
- Barbehenn RV, Karowe DN, Chen Z (2004) Performance of a generalist grasshopper on a C3 and a C4 grass: compensation for the effects of elevated CO₂ on plant nutritional quality. *Oecologia* 140:96–103
- Barkla BJ, Vera-Estrella R, Pantoja O, Kirch HH, Bohnert HJ (1999) Aquaporin localization—how valid are the TIP and PIP labels? *Trends Plant Sci* 4:86–88
- Benjamini Y, Hochberg Y (1995) Controlling the false discovery rate: a practical and powerful approach to multiple testing. *J Royal Stat Soc B* 57:289–300
- Benson D, Lipman DJ, Ostell J (1993) GenBank. *Nucleic Acids Res* 21:2963–2965
- Bootten TJ, Harris PJ, Melton LD, Newman RH (2004) Solid-state ¹³C-NMR spectroscopy shows that the xyloglucans in the primary cell walls of mung bean (*Vigna radiata* L.) occur in different domains: a new model for xyloglucan-cellulose interactions in the cell wall. *J Exp Bot* 55:571–583
- Breitling R, Armengaud P, Amtmann A, Herzyk P (2004) Rank products: a simple, yet powerful, new method to detect differentially regulated genes in replicated microarray experiments. *FEBS Lett* 573:83–92
- Busov VB, Meilan R, Pearce DW, Ma C, Rood SB et al (2003) Activation tagging of a dominant gibberellin catabolism gene (GA 2-oxidase) from poplar that regulates tree stature. *Plant Physiol* 132:1283–1291
- Canman JC, Hoffman DB, Salmon ED (2000) The role of pre- and post-anaphase microtubules in the cytokinesis phase of the cell cycle. *Curr Biol* 10:611–614
- Casler MD, Buxton DR, Vogel KP (2002) Genetic modification of lignin concentration affects fitness of perennial herbaceous plants. *Theor Appl Genet* 104:127–131
- Chen K, Hu GQ, Lenz F (2006) Effects of doubled atmospheric CO₂ concentration on apple trees. IV. Water consumption. CABI Abstract
- Conley MM, Kimball BA, Brooks TJ, Jr PP, Hunsaker DJ et al (2001) CO₂ enrichment increases water-use efficiency in sorghum. *New Phytol* 151:407–412
- Cooper KF, Strich R (2002) Saccharomyces cerevisiae C-type cyclin Ume3p/Srb11p is required for efficient induction and execution of meiotic development. *Eukaryot Cell* 1:66–74
- Cosgrove DJ (2000) Loosening of plant cell walls by expansins. *Nature* 407:321–326
- Darbah JNT, Kubiske ME, Nelson N, Kets K, Riikonen J et al (2010) Will photosynthetic capacity of forest trees acclimate after long-term exposure to elevated CO₂ and O₃? *Environ Pollut* 158:983–991
- Deprost D, Yao L, Sormani R, Moreau M, Leterreux G et al (2007) The Arabidopsis TOR kinase links plant growth, yield, stress resistance and mRNA translation. *EMBO Rep* 8:864–870
- Derbyshire P, McCann MC, Roberts K (2007) Restricted cell elongation in Arabidopsis hypocotyls is associated with a reduced average pectin esterification level. *BMC Plant Biol* 7:31
- Dickson RE, Lewin KF, JGEA Isebrands (2000) Forest atmosphere carbon transfer and storage (FACTS-II) the aspen free-air CO₂ and O₃ enrichment (FACE) project: an overview. U.S. Department of Agriculture, Forest Service, General Technical Report, NC-214, St. Paul, MN, USA
- Druart N, Rodriguez-Buey M, Barron-Gafford G, Sjodin A, Bhalerao R et al (2006) Molecular targets of elevated CO₂ in leaves and stems of *Populus deltoides*: implications for future tree growth and carbon sequestration. *Funct Plant Biol* 33:121–131
- Du J, Xie HL, Zhang DQ, He XQ, Wang MJ et al (2006) Regeneration of the secondary vascular system in poplar as a novel system to investigate gene expression by a proteomic approach. *Proteomics* 6:881–895
- Fukuzawa H, Yamano T (2005) Mechanism of CO₂-responsive transcriptional regulation in photosynthetic organisms: carbon-concentrating mechanism in a green alga, *Chlamydomonas reinhardtii*. *Tanpakushitsu Kakusan Koso* 50:958–965
- Ghanem ME, Albacete A, Smigocki AC, Frebort I, Pospisilova H et al (2011) Root-synthesized cytokinins improve shoot growth and fruit yield in salinized tomato (*Solanum lycopersicum* L.) plants. *J Exp Bot* 62:125–140
- Goujon T, Minic Z, El Amrani A, Lerouxel O, Aletti E et al (2003) AtBXL1, a novel higher plant (*Arabidopsis thaliana*) putative beta-xylosidase gene, is involved in secondary cell wall metabolism and plant development. *Plant J Cell Mol Biol* 33:677–690
- Gregory SL, Ebrahimi S, Milverton J, Jones WM, Bejsovec A et al (2008) Cell division requires a direct link between microtubule-bound RacGAP and Anillin in the contractile ring. *Curr Biol* 18:25–29
- Gupta P, Duplessis S, White H, Karnosky DF, Martin F et al (2005) Gene expression patterns of trembling aspen trees following long-term exposure to interacting elevated CO₂ and tropospheric O₃. *New Phytologist* 167:129–142
- Hamm-Alvarez SF, Sheetz MP (1998) Microtubule-dependent vesicle transport: modulation of channel and transporter activity in liver and kidney. *Physiol Rev* 78:1109–1129

- Herrero AB, Magnelli P, Mansour MK, Levitz SM, Bussey H et al (2004) KRE5 gene null mutant strains of *Candida albicans* are avirulent and have altered cell wall composition and hypha formation properties. *Eukaryot Cell* 3:1423–1432
- Hillstrom ML, Lindroth RL (2008) Elevated atmospheric carbon dioxide and ozone alter forest insect abundance and community composition. *Insect Conserv Divers* 1:233–241
- Hirose N, Makita N, Kojima M, Kamada-Nobusada T, Sakakibara H (2007) Overexpression of a type-A response regulator alters rice morphology and cytokinin metabolism. *Plant Cell Physiol* 48:523–539
- Irizarry RA, Hobbs B, Collin F, Beazer-Barclay YD, Antonellis KJ et al (2003) Exploration, normalization, and summaries of high density oligonucleotide array probe level data. *Biostatistics* 4:249–264
- Isebrand JG, McDonald EP, Kruger E, Hendrey G, Percy K et al (2001) Growth responses of *Populus tremuloides* clones to interacting elevated carbon dioxide and tropospheric ozone. *Environ Pollut* 115:359–371
- Ji P, Agrawal S, Diederichs S, Baumer N, Becker A et al (2005) Cyclin A1, the alternative A-type cyclin, contributes to G1/S cell cycle progression in somatic cells. *Oncogene* 24:2739–2744
- Joubes J, Lemaire-Chamley M, Delmas F, Walter J, Hernould M et al (2001) A new C-type cyclin-dependent kinase from tomato expressed in dividing tissues does not interact with mitotic and G1 cyclins. *Plant Physiol* 126:1403–1415
- Krizek BA (2009) Making bigger plants: key regulators of final organ size. *Curr Opin Plant Biol* 12:17–22
- Kubiske ME, Quinn VS, Marquardt PE, Karnosky DF (2007) Effects of elevated atmospheric CO₂ and/or O₃ on intra- and interspecific competitive ability of aspen. *Plant Biol (Stuttg)* 9:342–355
- Kutschera U (1990) Cell wall synthesis and elongation growth in hypocotyls of *Helianthus annuus* (L.). *Planta* 181:316–323
- Larkin K, Danilchik MV (1999) Microtubules are required for completion of cytokinesis in sea urchin eggs. *Dev Biol* 214:215–226
- Leakey AD, Ainsworth EA, Bernacchi CJ, Rogers A, Long SP et al (2009) Elevated CO₂ effects on plant carbon, nitrogen, and water relations: six important lessons from FACE. *J Exp Bot* 60:2859–2876
- Lefebvre S, Lawson T, Zakhleniuk OV, Lloyd JC, Raines CA et al (2005) Increased sedoheptulose-1,7-bisphosphatase activity in transgenic tobacco plants stimulates photosynthesis and growth from an early stage in development. *Plant Physiol* 138:451–460
- Li F, Kang S, Zhang F (2003) Effects of CO₂ enrichment, nitrogen and water on photosynthesis, evapotranspiration and water use efficiency of spring wheat. *Ying Yong Sheng Tai Xue Bao* 14:387–393
- Li QM, Liu BB, Wu Y, Zou ZR (2008) Interactive effects of drought stresses and elevated CO₂ concentration on photochemistry efficiency of cucumber seedlings. *J Integr Plant Biol* 50:1307–1317
- Liu L, King JS, Giardina CP (2005) Effects of elevated concentrations of atmospheric CO₂ and tropospheric O₃ on leaf litter production and chemistry in trembling aspen and paper birch communities. *Tree Physiol* 25:1511–1522
- Liu N, Lu M, Tian X, Han Z (2006) Molecular mechanisms involved in self-renewal and pluripotency of embryonic stem cells. *J Cell Physiol* 221:279–286
- Liu LL, King JS, Giardina CP, Booker FLFL (2009) The Influence of chemistry, production and community composition on leaf litter decomposition under elevated atmospheric CO₂ and Tropospheric O₃ in a northern hardwood ecosystem. *Ecosystems* 12:401–416
- Ma QH (2007) Small GTP-binding proteins and their functions in plants. *J Plant Growth Regul* 26:369–388
- Macdonald B (1986) Practical woody plant propagation for nursery growers. Timber Press, Inc., Portland
- Maeshima M (2001) TONOPLAST TRANSPORTERS: organization and Function. *Annu Rev Plant Physiol Plant Mol Biol* 52:469–497
- Meyer RC, Steinfath M, Lisec J, Becher M, Witucka-Wall H et al (2007) The metabolic signature related to high plant growth rate in *Arabidopsis thaliana*. *Proc Natl Acad Sci USA* 104:4759–4764
- Muto E, Sakai H, Kaseda K (2005) Long-range cooperative binding of kinesin to a microtubule in the presence of ATP. *J Cell Biol* 168:691–696
- Nakashima A, Maruki Y, Imamura Y, Kondo C, Kawamata T et al (2008) The yeast Tor signaling pathway is involved in G2/M transition via polo-kinase. *PLoS ONE* 3:e2223
- Nielsen TH, Rung JH, Villadsen D (2004) Fructose-2,6-bisphosphate: a traffic signal in plant metabolism. *Trends Plant Sci* 9:556–563
- Nieminen K, Immanen J, Laxell M, Kauppinen L, Tarkowski P et al (2008) Cytokinin signaling regulates cambial development in poplar. *Proc Natl Acad Sci USA* 105:20032–20037
- Okamoto M, Kuwahara A, Seo M, Kushiro T, Asami T et al (2006) CYP707A1 and CYP707A2, which encode abscisic acid 8'-hydroxylases, are indispensable for proper control of seed dormancy and germination in *Arabidopsis*. *Plant Physiol* 141:97–107
- Okamoto M, Kushiro T, Jikumaru Y, Abrams SR, Kamiya Y et al (2011) ABA 9'-hydroxylation is catalyzed by CYP707A in *Arabidopsis*. *Phytochemistry* 72:717–722
- Orcutt DM, Nilsen ET, Hale MG (2000) The physiology of plants under stress: soil and biotic factors. Wiley, New York
- Persson S, Wei H, Milne J, Page G, Somerville C (2005a) Identification of genes required for cellulose synthesis by regression analysis of public microarray data sets. *Proc Natl Acad Sci USA* 102:8633–8638
- Persson S, Wei H, Milne J, Page GP, Somerville CR (2005b) Identification of genes required for cellulose synthesis by regression analysis of public microarray data sets. *Proc Natl Acad Sci USA* 102:8633–8638
- Pregitzer KS, Burton AJ, King JS, Zak DR (2008) Soil respiration, root biomass, and root turnover following long-term exposure of northern forests to elevated atmospheric CO₂ and tropospheric O₃. *New Phytol* 180:153–161
- Schnitzer MJ, Block SM (1997) Kinesin hydrolyses one ATP per 8-nm step. *Nature* 388:386–390
- Smith HB (1999) Constructing signal transduction pathways in *Arabidopsis*. *Plant Cell* 11:299–301
- Surka MC, Tsang CW, Trimble WS (2002) The mammalian septin MSF localizes with microtubules and is required for completion of cytokinesis. *Mol Biol Cell* 13:3532–3545
- Takahashi K, Mitsui K, Yamanaka S (2003) Role of ERas in promoting tumour-like properties in mouse embryonic stem cells. *Nature* 423:541–545
- Tamoi M, Nagaoka M, Miyagawa Y, Shigeoka S (2006) Contribution of fructose-1,6-bisphosphatase and sedoheptulose-1,7-bisphosphatase to the photosynthetic rate and carbon flow in the Calvin cycle in transgenic plants. *Plant Cell Physiol* 47:380–390
- Taylor G, Street NR, Tricker PJ, Sjodin A, Graham L et al (2005) The transcriptome of *Populus* in elevated CO₂. *New Phytol* 167:143–154
- Thomas BR, Rodriguez RL (1994) Metabolite signals regulate gene expression and source/sink relations in cereal seedlings. *Plant Physiol* 106:1235–1239
- Tiwari SB, Wang XJ, Hagen G, Guilfoyle TJ (2001) AUX/IAA proteins are active repressors, and their stability and activity are modulated by auxin. *Plant Cell* 13:2809–2822

- Tiwari SB, Hagen G, Guilfoyle TJ (2004) Aux/IAA proteins contain a potent transcriptional repression domain. *Plant Cell* 16:533–543
- To JP, Deruere J, Maxwell BB, Morris VF, Hutchison CE et al (2007) Cytokinin regulates type-A Arabidopsis Response Regulator activity and protein stability via two-component phosphorelay. *Plant Cell* 19:3901–3914
- Trivedi P, Edwards JW, Wang J, Gadbury GL, Srinivasasainagendra V et al (2005) HDBStat!: a platform-independent software suite for statistical analysis of high dimensional biology data. *BMC Bioinform* 6:86
- Tuba Z, Lichtenthaler HK (2007) Long-term acclimation of plants to elevated CO₂ and its interaction with stresses. *Ann N Y Acad Sci* 1113:135–146
- Tuskan GA, Difazio S, Jansson S, Bohlmann J, Grigoriev I et al (2006) The genome of black cottonwood, *Populus trichocarpa* (Torr. & Gray). *Science* 313:1596–1604
- Uddling J, Teclaw RM, Kubiske ME, Pregitzer KS, Ellsworth DS (2008) Sap flux in pure aspen and mixed aspen-birch forests exposed to elevated concentrations of carbon dioxide and ozone. *Tree Physiol* 28:1231–1243
- Uematsu K, Suzuki N, Iwamae T, Inui M, Yukawa H (2012) Increased fructose 1,6-bisphosphate aldolase in plastids enhances growth and photosynthesis of tobacco plants. *J Exp Bot* 63:3001–3009
- Welters P, Takegawa K, Emr SD, Chrispeels MJ (1994) AtVPS34, a phosphatidylinositol 3-kinase of *Arabidopsis thaliana*, is an essential protein with homology to a calcium-dependent lipid binding domain. *Proc Nat Acad Sci USA* 91:11398–11402
- Yang Z (2002) Small GTPases: versatile signaling switches in plants. *Plant Cell* 14(Suppl):S375–S388
- Yu Y, Steinmetz A, Meyer D, Brown S, Shen WH (2003) The tobacco A-type cyclin, Nicta;CYCA3;2, at the nexus of cell division and differentiation. *Plant Cell* 15:2763–2777
- Zaragoza D, Ghavidel A, Heitman J, Schultz MC (1998) Rapamycin induces the G0 program of transcriptional repression in yeast by interfering with the TOR signaling pathway. *Mol Cell Biol* 18:4463–4470
- Zdobnov EM, Apweiler R (2001) InterProScan—an integration platform for the signature-recognition methods in InterPro. *Bioinformatics* 17:847–848
- Zhong R, Lee C, Zhou J, McCarthy RL, Ye ZH (2008) A battery of transcription factors involved in the regulation of secondary cell wall biosynthesis in *Arabidopsis*. *Plant Cell* 20:2763–2782